Crystallographic and magnetic identification of secondary phase in orientated Bi5Fe0.5Co0.5Ti3O15 ceramics

Meghdad Palizdar, Tim P. Comyn, Michael B. Ward, Andrew P. Brown, John P. Harrington et al.

Citation: J. Appl. Phys. **112**, 073919 (2012); doi: 10.1063/1.4754562
View online: http://dx.doi.org/10.1063/1.4754562
View Table of Contents: http://jap.aip.org/resource/1/JAPIAU/v112/i7
Published by the American Institute of Physics.

Crystallographic and magnetic identification of secondary phase in orientated $Bi_5Fe_{0.5}Co_{0.5}Ti_3O_{15}$ ceramics

Meghdad Palizdar,[1] Tim P. Comyn,[1,a)] Michael B. Ward,[1] Andrew P. Brown,[1] John P. Harrington,[1] Santosh Kulkarni,[2] Lynette Keeney,[2] Saibal Roy,[2] Martyn Pemble,[2] Roger Whatmore,[2] Christopher Quinn,[3] Susan H. Kilcoyne,[4] and Andrew J. Bell[1]
[1]*Institute for Materials Research, SPEME, University of Leeds, LS2 9JT Leeds, United Kingdom*
[2]*Tyndall National Institute, University College Cork, 'Lee Maltings', Dyke Parade, Cork, Ireland*
[3]*Institute for Materials Research, University of Salford, M5 4WT Salford, United Kingdom*
[4]*School of Applied Science, University of Huddersfield, Queens Gate, Huddersfield HD1 3DH, United Kingdom*

(Received 19 May 2012; accepted 24 August 2012; published online 8 October 2012)

The fabrication of highly-oriented polycrystalline ceramics of $Bi_5Fe_{0.5}Co_{0.5}Ti_3O_{15}$, prepared via molten salt synthesis and uniaxial pressing of high aspect ratio platelets is reported. Electron backscatter images show a secondary phase within the ceramic which is rich in cobalt and iron. The concentration of the secondary phase obtained from scanning electron microscopy is estimated at less than 2% by volume, below the detection limit of x-ray diffraction (XRD). The samples were characterized by x-ray diffraction, polarization-electric field measurements, superconducting quantum interference device as a function of sample orientation and vibrating sample magnetometry as a function of temperature. It is inferred from the data that the observed ferromagnetic response is dominated by the secondary phase. This work highlights the importance of rigorous materials characterisation in the study of multiferroics as small amounts of secondary phase, below the limit of XRD, can lead to false conclusions. © *2012 American Institute of Physics*. [http://dx.doi.org/10.1063/1.4754562]

I. INTRODUCTION

There has recently been great interest in identifying multiferroic materials, which simultaneously exhibit both ferroelectric and magnetic order. However, room temperature examples are rather rare due to the mutually exclusive nature of the electron configurations normally associated with the transition metal cations in simple ferroelectrics and ferromagnets.[1] The perovskite $BiFeO_3$,[2] for example, has engendered many studies as it is ferroelectric and antiferromagnetic at room temperature, however it is not ferromagnetic.

Aurivillius[3] compounds, with the general formula $A_{m+1}Bi_2M_mO_{3m+3}$, are of interest in this context as their layer structure potentially provides an opportunity to separate the cations responsible for ferroelectricity and ferromagnetism, respectively, into the two different sub-structures of the crystal, thereby allowing the two electronic configuration conditions to exist in the same crystal. The structure can be described as layers comprising *m* simple unit cells of perovskite $[A_{m-1}B_mO_{3m+1}]^{2-}$, sandwiched between rock salt structure layers of $(Bi_2O_2)^{2+}$.

As $Bi_4Ti_3O_{12}$ is itself ferroelectric,[4] it has been conjectured that the Aurivillius compounds of general formula, $(BiFeO_3)_{n-1}Bi_4Ti_3O_{12}$, could include materials that are ferroelectric-ferromagnets. $Bi_5Ti_3FeO_{15}$, $Bi_6Ti_3Fe_2O_{18}$, and $Bi_9Ti_3Fe_5O_{27}$ were reported by Ismailzade *et al.*[5] and were shown to be antiferromagnetic with their Néel temperatures increasing with the value of *m*.

For the n = 2 compound it was recently shown that both ferroelectric and ferromagnetic properties are exhibited at room temperature for compositions in which half the Fe^{3+} ions are replaced by Co^{3+}, ($Bi_5Fe_{0.5}Co_{0.5}Ti_3O_{15}$) referred to here as BFCT. Values of 7.8 memu/g and 410 Oe for remanent magnetization ($2M_r$) and coercive field ($2H_c$), respectively, were reported for ceramics synthesized by a multi-calcination procedure, with a magnetic Curie temperature of 345 °C.[6] This result is significant as this material would be the only currently-known material that is both ferroelectric and ferromagnetic at room temperature.

One of the drawbacks of carrying out studies of multiferroic materials in conventional polycrystalline ceramic form is that the key properties arising from the ferroic order, the electrical polarization and magnetisation, are rendered isotropic in unpoled materials, while in poled materials information relating to the true symmetry properties are lost. While growth of single crystals is obviously the preferred route to obtain unambiguous symmetry related property data, this is often a complex and time consuming route. The preparation of "textured" or "grain-oriented" polycrystalline materials which exhibit preferred crystallographic orientation, can on the one hand provide useful symmetry related property data more efficiently than single crystals and on the other hand can provide a cost effective route to the manufacture of materials with enhanced properties compared to those of random oriented materials. In such materials, one would expect ferroic orders to be anisotropic, thereby allowing the correlation of any experimental observation with preferred orientation.

In this present work, a molten salt synthesis method has been employed to produce grain-oriented ceramics of BFCT

a)t.p.comyn@leeds.ac.uk.

in order to provide greater insight into the ferroelectric and magnetic properties of the material. The results were compared to the BFCT made via a conventional method.

II. EXPERIMENTAL

The molten salt method was employed to synthesize platelets of BFCT from a chloride flux. The constituent oxide powders, Bi_2O_3, TiO_2, Fe_2O_3 and Co_2O_3 (purity, 99.9%, Aldrich, Germany) were mixed in stoichiometric quantities with respect to $Bi_5Fe_{0.5}Co_{0.5}Ti_3O_{15}$ by ball milling with zirconia balls in iso-propanol for 24 h. After drying, the powders were ground through a 100 mesh sieve to reduce the aggregate size. An equal weight of 1:1 mole ratio NaCl:KCl was added and mixed with the oxide powders using an agate pestle and mortar. The resulting mixture was placed into an alumina crucible and heated to 1000 °C at a rate of 300 °C h^{-1}, with a 1 h dwell at temperature, then cooled at a rate of 150 °C h^{-1} to room temperature. The products were crushed and repeatedly washed with hot de-ionized water to remove the salts from the mixture. For comparison, a conventional solid state reaction process was also used to prepare powders, by calcining the mixed oxide precursors at 640 °C for 8 h before further die pressing.[6]

The resulting powders, prepared by both methods, were pressed into pellets at 120 MPa, followed by sintering at a range of different temperatures, in order to optimise the density of the fired materials. The conventionally-prepared powders were sintered for 6 h at 850 °C, similar to reference,[6] whereas optimum density for the molten salt prepared powders was obtained at 1000 °C for 1 h. The materials were characterized using scanning electron microscopy(SEM), using a Zeiss Leo (Field Emission Gun)-SEM (Carl Zeiss SMT Ltd., Cambridge, United Kingdom), and transmission electron microscopy (TEM), by using FEI Tecnai TF20 FEG-TEM, x-ray powder diffraction on a PANalytical X'Pert MPD system (Almelo, the Netherlands), vibrating sample magnetometry (VSM) and superconducting quantum interference device (SQUID) magnetometry. The Oxford instruments model VSM was used. The VSM allows measurements in the temperature range of −223 °C to 727 °C and can generate an applied magnetic field from −30 000 up to +30 000 Oe using a helium compressed cryogenic magnet system. Room temperature magnetic measurements were carried out using a SQUID magnetometer (superconducting quantum interference device, Quantum Design USA; Model-MPMS XL5) over an applied magnetic field range of ±5000 Oe. Also, to prepare samples for TEM, an FEI Nova 200 NanoLab high resolution field emission gun scanning electron microscope (FEGSEM) with precise focused ion beam (FIB) was used.

III. RESULTS

Fig. 1(a) shows BFCT crystallites made via the conventional method and calcined at 640 °C for 8 h followed by sintering at 850 °C for 6 h. Fig. 1(b) shows the morphology of BFCT crystallites prepared at 1000 °C for 1 h by the molten salt method. The crystallites possess a platelet form, Fig. 1(b), with a high aspect ratio: thickness ≈ 0.2 μm, and lateral

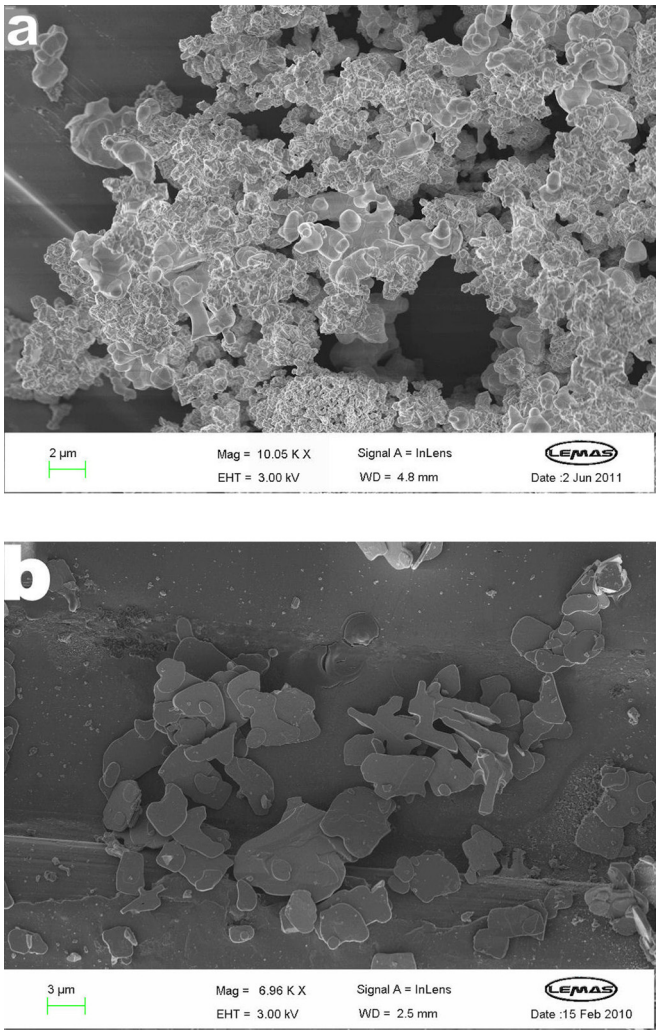

FIG. 1. (a) SEM image of $Bi_5Fe_{0.5}Co_{0.5}Ti_3O_{15}$ prepared at 640 °C for 8 h, and followed by sintering at 850 °C for 6 h, (conventional method) and (b) $Bi_5Fe_{0.5}Co_{0.5}Ti_3O_{15}$ powders prepared at 1000 °C for 1 h (molten salt method.)

width 2–20 μm, whereas particles obtained from the conventional method are agglomerated without any plate like morphology.

Fig. 2 show the results of x-ray powder diffraction employing conventional Bragg-Brentano geometry on ceramics prepared from the two different particle preparation routes. Fig. 2(a) is similar to that published by Mao *et al.*[6] for the BFCT prepared by the conventional mixed oxide process. Fig. 2(b) shows evidence of strong crystallographic preferred orientation with the (00*l*) planes lying parallel to the ceramic surface i.e., normal to the direction of the application of pressure during the uniaxial pressing process. To estimate the degree of orientation, the Lotgering factor,[7] *f*, was calculated using the following formula

$$f = \frac{P - P_0}{1 - P_0}, \tag{1}$$

where

$$P = \frac{\Sigma I(00l)}{\Sigma I(hkl)}, \tag{2}$$

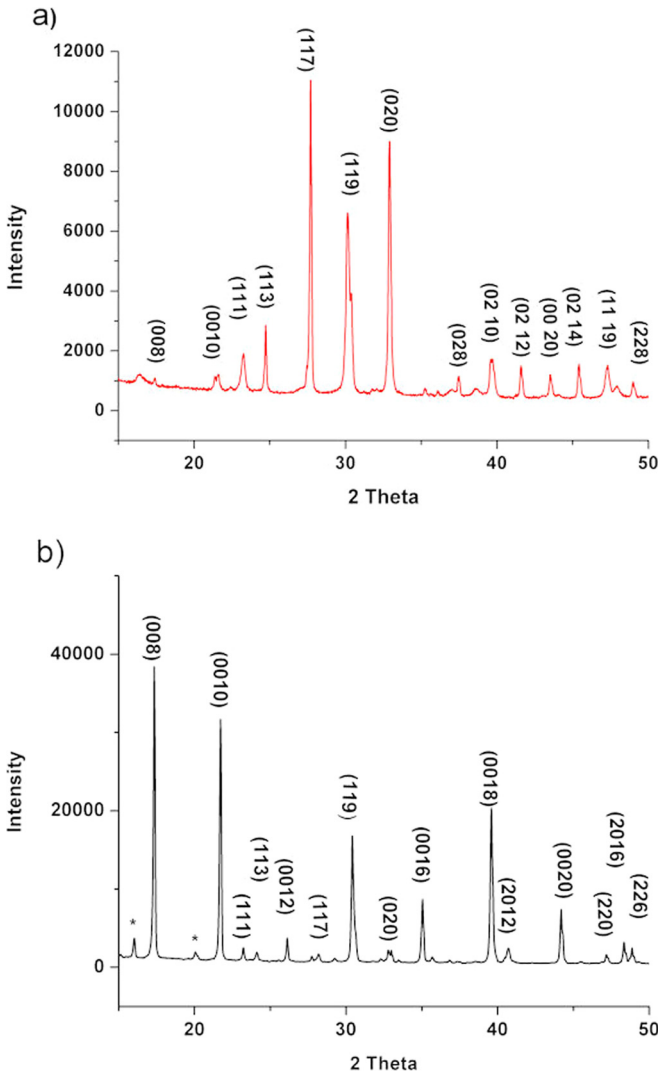

FIG. 2. X-ray diffraction patterns of BFCT powders prepared by (a) conventional mixed oxide processing and (b) by the molten salt method.

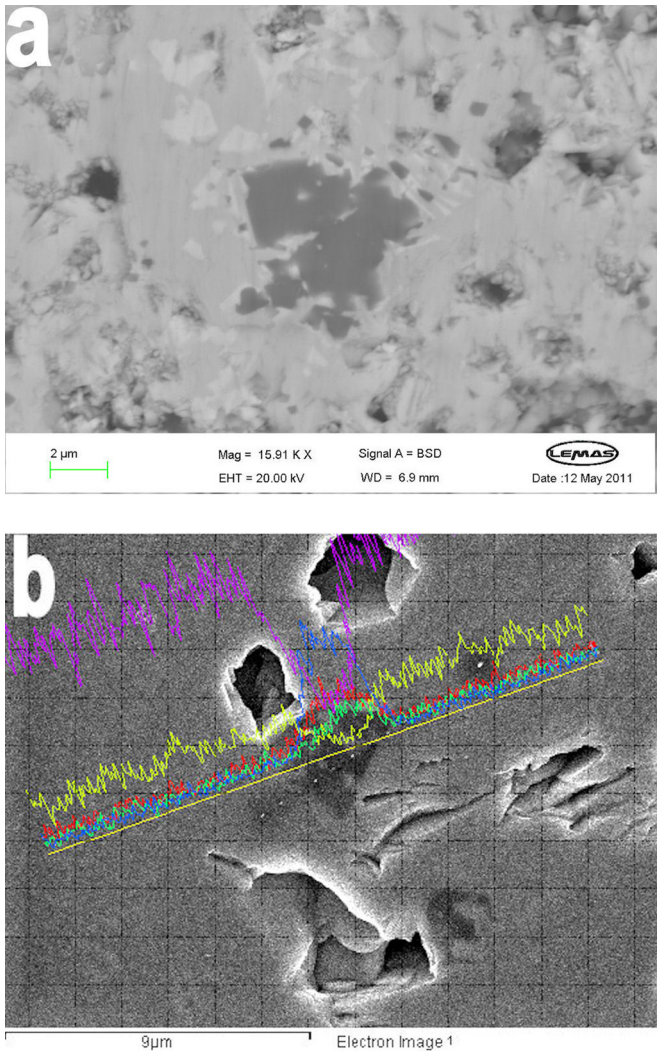

FIG. 3. EBS image of BFCT pellet prepared from (a) conventional method and (b) molten salt method at 1000 °C for 1 h, showing a region of suspected second phase.

and $P_0 = P$ for a randomly oriented material with $I(00l)$ and $I(hkl)$ being the intensities of the relevant (hkl). Full texture is indicated when $f = 1$ and random texture when $f = 0$. The Lotgering factor for BFCT obtained from molten salt method was $f = 0.695$, whereas using conventional method, $f = 0.115$, showing that a high degree of texturing has been achieved via molten salt method. Note that P_0 was calculated via theoretical (hkl) intensities obtained by CRYSTALLOGRAPHICA software.

Fig. 3 shows electron backscatter (EBS) images of 0.5 μm polished sections through BFCT pellets prepared by both conventional and molten salt synthesis methods. Backscattered electrons are elastically scattered, hence the resulting image is sensitive to the atomic number contrast, and therefore ideal for searching for possible secondary phases. High atomic number regions appear bright, and conversely low numbers appear dark. Discrete dark areas are observed in Fig. 3, suggesting regions of low atomic number.[8] EBS images of BFCT prepared from the conventional solid state reaction method displayed the existence of a secondary phase (Fig. 3(a)). Image analysis of a relatively large area of sample, synthesised by molten salt, approximately 800 μm^2, also indicates the presence of secondary phase with a volume fraction of approximately 2%, as estimated from the area fraction (Fig. 3(b)), calculated by AxioVision image processing software. Image analysis for BFCT prepared by conventional method showed a much lower amount of secondary phase, which was difficult to quantify, but was estimated at 0.15% by volume.

In order to identify the composition of these regions, energy dispersive x-ray analysis (EDX) was employed in the form of a line scan, (Fig. 4) across one of the dark regions over the sample made via molten salt method (Fig. 3(b)). These scans show that the darker area is rich in Co and Fe, with little evidence of the presence of bismuth and titanium. However, SEM EDX spot scan analysis on some parts of dark regions in Fig. 3(b), suggests the existence of considerable amount of Ti in some parts of secondary phase (Table I). The main phase comprises of bismuth, titanium and iron and the EDX results suggest a very low concentration of Co.

To help identify the secondary phase, electron diffraction was carried out on thin sections prepared by a FIB

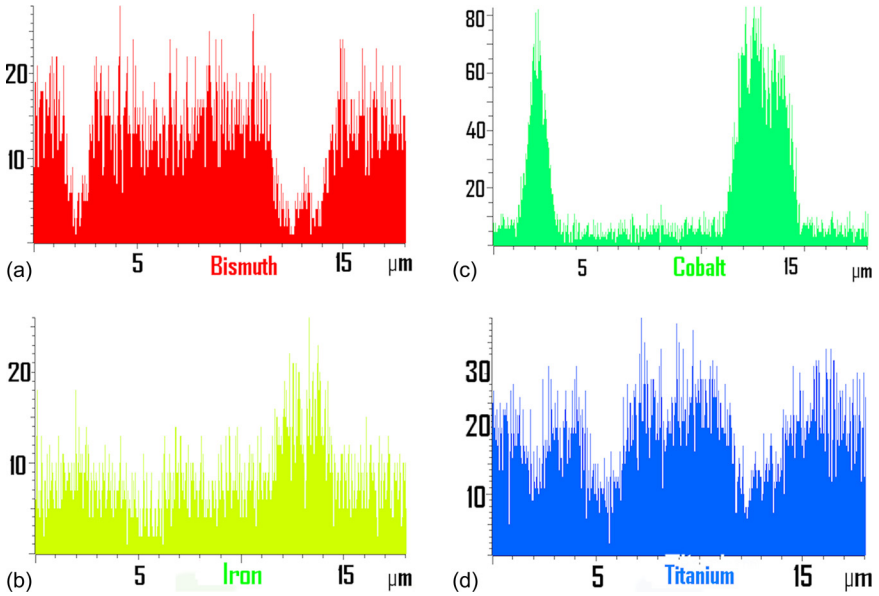

FIG. 4. EDX elemental line-scans across the suspected secondary phase, Fig. 3(b), from the sample made via molten salt method.

microscope[9] so as to include a region of the secondary phase, as shown in Fig. 5. The darker area represents the secondary phase. Fig. 6 shows a selected area electron diffraction pattern for the secondary phase. The pattern matches ICSD file 00-022-1086, for cobalt ferrite ($CoFe_2O_4$) which is a cubic inverse spinel with a lattice parameter of 8.3919 Å. However, in agreement with the SEM EDX data, the TEM EDX analysis confirms the existence of the Ti in the secondary phase (Table II), therefore the secondary phase is thought to be a substituted normal spinel of composition $Co_2Fe_{1-x}Ti_xO_4$.

SQUID measurements for BFCT prepared in this study by the conventional solid state reaction method give a remanent magnetization of 2.5 memu/g for random BFCT crystals (Fig. 7). Furthermore, SQUID magnetometry was used to compare the M-H (magnetization vs. applied magnetic field) at room temperature for samples in which the magnetic field was parallel (in-plane) and perpendicular (out-of-plane) to the preferred c-axis of the oriented BFCT pellet sample (prepared by molten salt synthesis); the data are shown in Fig. 8. The coercivity is approximately 350 Oe, with a remanent magnetization of 72.5 memu/gm (out-of-plane) and 77 memu/gm (in-plane). The M-H loops confirm the existence of a ferromagnetic phase within the material, however, the inability to saturate the sample even at a field of 5 T, suggests the presence of additional magnetic phases. The in-plane magnetization values of BFCT produced from the molten salt method is approximately ten times greater than that reported for BFCT by Mao *et al.*,[6] which was made from a conventional solid state reaction method.

TABLE I. Spot scan SEM EDX data from secondary phase area of the sample made via molten salt process. The area of the scan shown as a dot in Fig. 3(b).

Elements	O	Co	Fe	Ti
At. %	58.9	22.9	10.9	7.2

The presence of the multiple magnetic phases within the sample was further confirmed from the magnetization vs temperature measurements. Fig. 9 shows the magnetization measurements by VSM for BFCT pellet made from the molten salt method, at different temperatures. On increasing the temperature, the remanent magnetization drops from approximately 77 memu/g at room temperature to 7.5 memu/g at 700 °C. VSM was run for both in-plane and out-of-plane orientation of the BFCT and the results were similar. The magnetic moment appears to gradually reduce with increasing temperature, while never completely reaching zero. This may suggest the presence of additional magnetic phases with higher Curie temperatures, as the main BFCT phase is reported to possess a Curie temperature of 345 °C.[6]

Figs. 10(a) and 10(b) show room temperature P-E hysteresis loop of BFCT pellet made from conventional and molten salt method, measured at 10 Hz with a different applied electrical field. Fig. 10(a) displays the remanent polarization of $2Pr \approx 12\,\mu C/cm^2$ at 11 kV/mm, approximately. The hysteresis loop could not be saturated and the sample experienced breakdown at higher field rather than 11 kV/mm, which suggests that the sample was below its coercive field. Furthermore, Fig. 10(a) shows a high level of leakage, from dc conductivity. However, the leakage is far lower in a material synthesised by molten salt process (Fig. 10(b)). Figs. 11(a) and 11(b) show the room temperature strain-electric field results for BFCT made from both conventional and molten salt methods, respectively, measured at 10 Hz. Strain-field result for conventional BFCT (Fig. 11(a)) represents the ferroelectric butterfly loop, whereas Fig. 11(b) suggests more electrostriction phenomenon for BFCT synthesised from molten salt method.

IV. DISCUSSION

X-ray diffraction (XRD) and SEM data confirm the existence of highly textured BFCT synthesised by the molten salt method. However, EBS images suggest the existence of

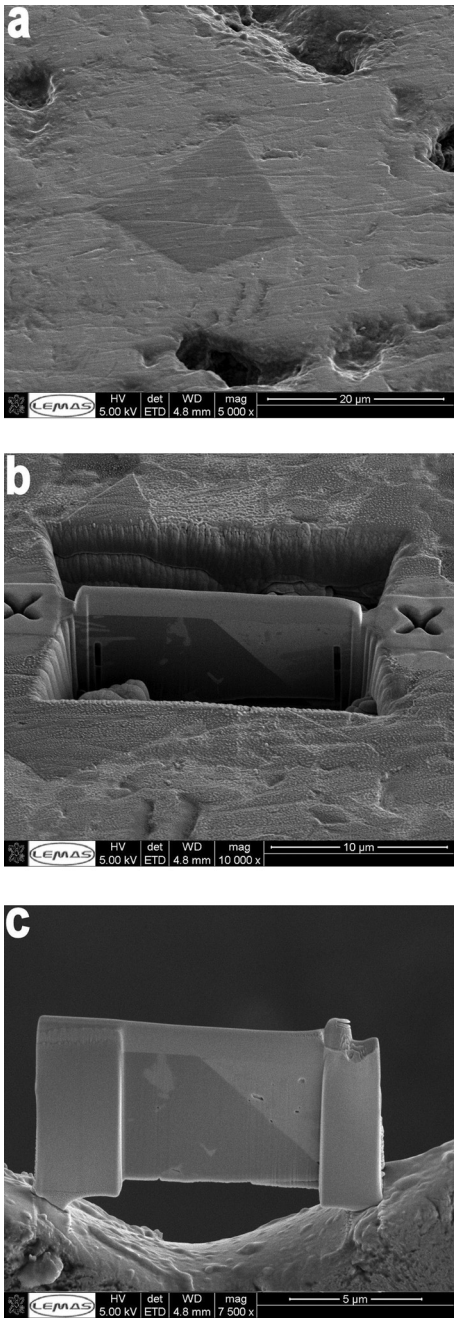

FIG. 5. (a) SEM electron image of the surface of the BFCT pellet prepared by the molten salt route, showing a dark area indicating the presence of the second phase; (b) FIB thin section cut through the secondary phase; (c) the thin section containing the secondary phase after lift-out and mounting on a TEM grid.

the secondary phase in both samples made by conventional and molten salt processes.

Based on EBS images, the amount of secondary phase in the sample made by the conventional method is less in comparison with the sample made by molten salt method. It has previously been reported that a Co and Fe rich phase may be formed at high temperature.[10] Consequently, there is more possibility for the Co and Fe rich secondary phase to form in the molten salt method due to the higher sintering temperature, 1000 °C, in comparison with conventional method which was only 850 °C. Consequently, more secondary phase exists in BFCT prepared by the molten salt method which results in the ceramic having a higher remanent magnetization.

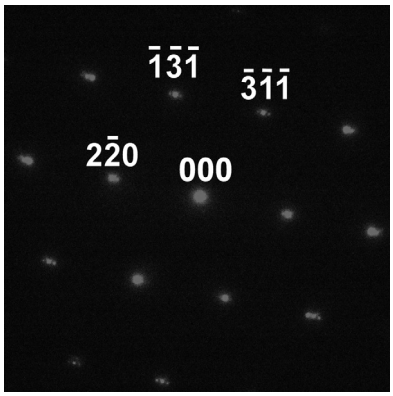

FIG. 6. Electron diffraction pattern from the secondary phase indexed to the [1 1 4] zone axis of a reference pattern of $CoFe_2O_4$ in BFCT pellet prepared by the molten salt method.

Based on TEM electron diffraction pattern and EDX chemical data, it can be concluded that the secondary phase is rich in Co and Fe. While Co_2FeO_4 is a normal spinel, and $CoFe_2O_4$ is an inverse spinel i.e., they have the same structure but different cation distributions (for more details see Refs. 11 and 12). The unit cell dimensions between the two systems are not very different (8.24 Å for Co_2FeO_4 and 8.39 Å for $CoFe_2O_4$) so electron diffraction would not be able to distinguish them (normally ~10% error should be accounted for when calculating *d*-spacings from electron diffraction due to the optics of the instrumentation). Furthermore, Tables I and II suggest the existence of Ti in the Co and Fe rich secondary phase, Therefore, the magnetic impurities have a Co_2FeO_4 type spinel structure with some titanium substitution of the iron. This redistribution has been shown to be possible for $CoFe_{2-x}Ti_xO_4$.[13]

Moreover, the impurity phase cannot be detected using XRD, even under very slow scan rates around the angles expected for the most intense diffraction peaks.

In summary, an electron diffraction pattern that can be indexed to a CoFe spinel lying with its [114] axis parallel to the electron beam was shown in Fig. 6 and used to calculate the lattice parameter for the secondary phase.

We would anticipate that if the textured Aurivillius structure was indeed magnetic, then the resultant magnetic response would be heavily influenced by orientation, unless the magnetic ordering was oriented at 45° to both the in-plane and out-of-plane direction, which seems highly unlikely. However, the absence of anisotropy in the magnetic properties (Fig. 7), suggests the possibility that the randomly oriented Co–Fe spinel phase dominates the ferromagnetic response of the sample. We can infer from this that the

TABLE II. TEM EDX data from secondary phase area which belonges to the sample made from molten salt method.

Elements	O	Co	Fe	Ti
At. %	64.4	28.5	5.1	1.9

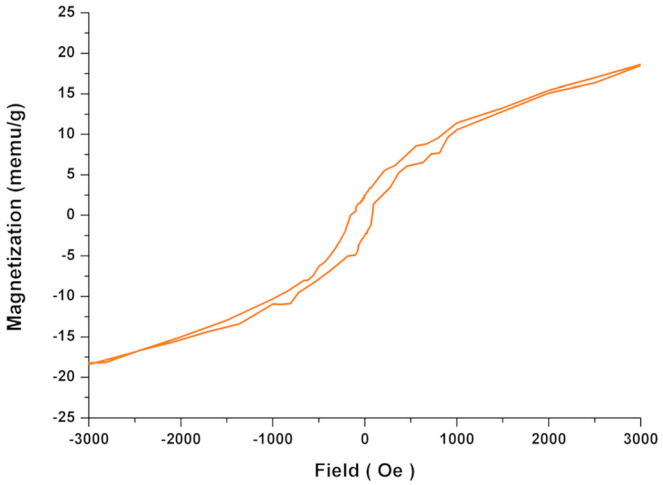

FIG. 7. M vs H loops for BFCT pellet, made from conventional method.

observed ferromagnetic properties for of the ceramics can be attributed solely to the Co/Fe rich secondary phases, rather than the $Bi_5Ti_3Fe_{0.5}Co_{0.5}O_{15}$ main phase.

$CoFe_2O_4$ is a ferromagnetic material with Curie temperature around 520 °C.[14] Co_2FeO_4 is a ferromagnetic material with a Curie temperature of 187 °C.[15] The magnetic properties of both strongly depend on cobalt and iron content, particle size, preparation method and particle shape.[16–18] The remanent magnetizations of $CoFe_2O_4$ and Co_2FeO_4 lie between 25 and 60 emu/g and 18–24 emu/g respectively,[19,20] and can reach 120 emu/cm^3 for $CoFe_2O_4$ thin films.[21]

Depending on the grain size, magnetic Curie temperature ranges of 520 °C–557 °C and 187 °C have been identified for $CoFe_2O_4$ and Co_2FeO_4, respectively.[14,15,22–24] Mao *et al.*[6] claimed a Curie temperature of 345 °C for BFCT. Consequently, by investigating the Curie temperature of BFCT prepared in this study, it would be possible to identify the influence of the $CoFe_2O_4$ secondary phase on the magnetic properties of the main BFCT phase. However, the results of magnetic measurements as a function of temperature shown in Fig. 9 show the presence of magnetic moment in the sample at the expected T_c for the Aurivillius phase or the $CoFe_2O_4/Co_2FeO_4$ spinel phases. One possible reason

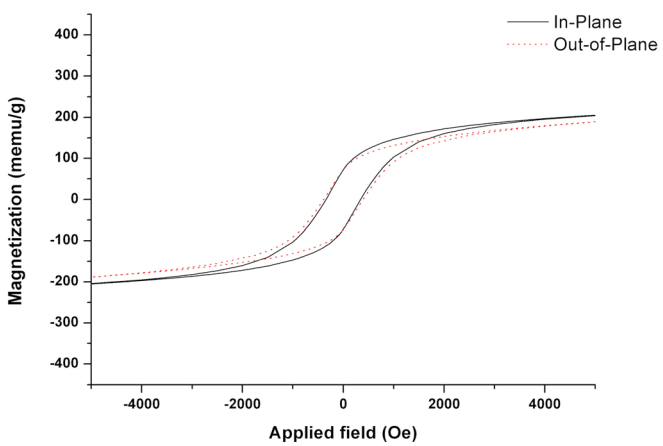

FIG. 8. Comparison of M vs H loops for grain oriented BFCT pellets, made by molten salt method with magnetic field perpendicular (in-plane) and parallel (out-of-plane) to the preferred c-axis.

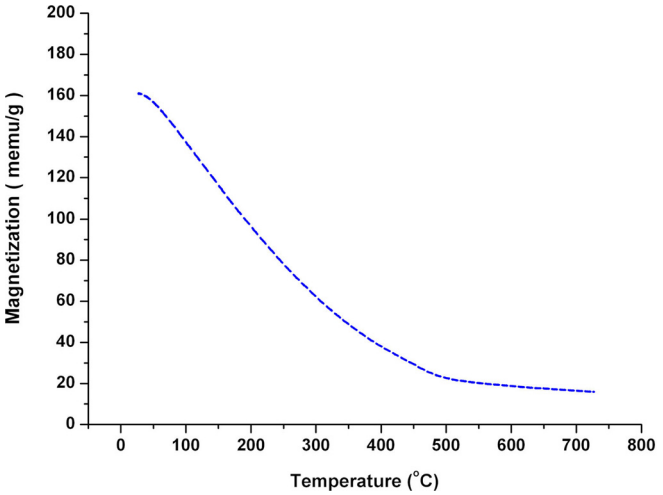

FIG. 9. M vs temperature results for BFCT pellet prepared by molten salt method at temperatures from RT to 740 °C.

could be the partial substitution of Fe by Ti which could account for the observed change in Curie temperature for the Co and Fe rich secondary phase. As mentioned earlier the secondary phase possesses a Co_2FeO_4 type spinel structure with some titanium substitution of the iron ($CoFe_{2-x}Ti_xO_4$).

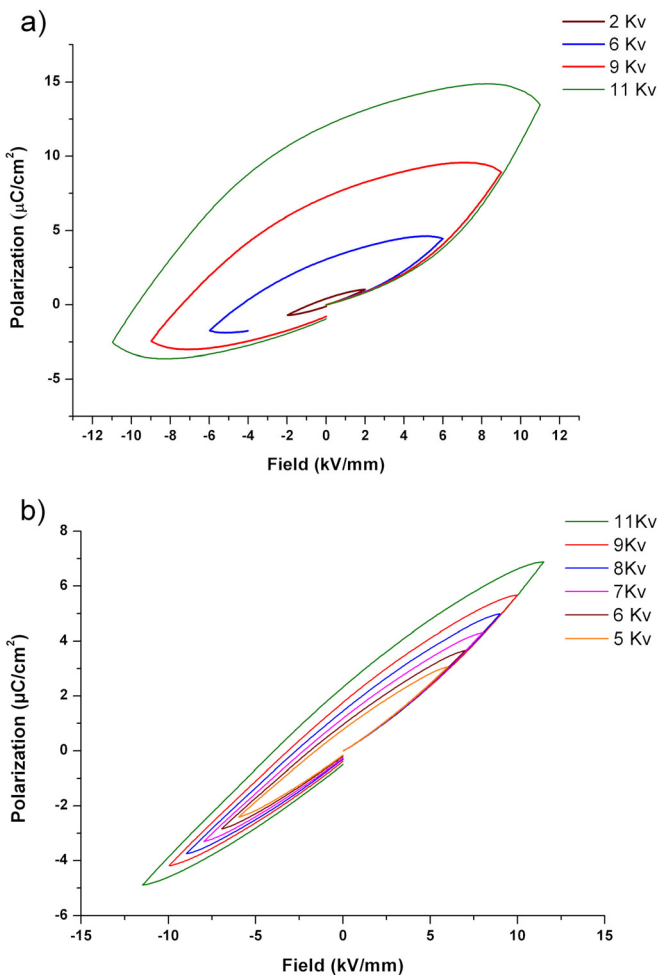

FIG. 10. Room temperature ferroelectric hysteresis loops for the textured BFCT pellets prepared by the (a) conventional solid state reaction and (b) molten salt method process.

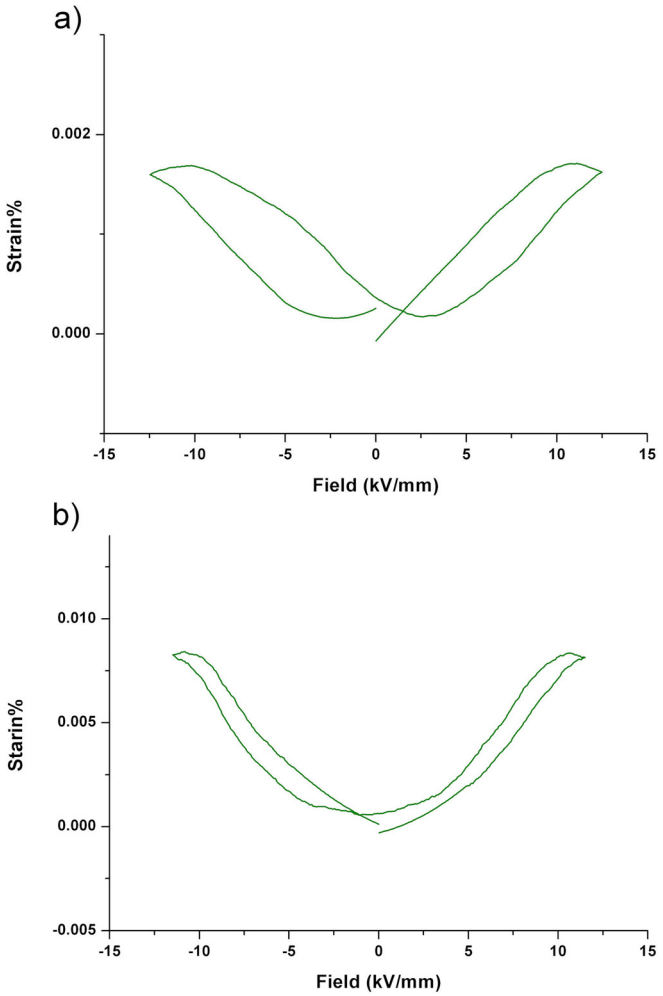

FIG. 11. Room temperature strain-field loops for the textured BFCT pellets prepared by the (a) conventional solid state reaction process and (b) molten salt method.

It is conceivable that the composition may have deviated from this without influencing the observed spinel structure, but with a large effect on the Curie temperature.

The Co and Fe rich secondary phase could have magnetization values anywhere between 18 and 60 emu/g,[19,20] therefore 2% by volume would contribute to the value of 75 memu/g, observed in the SQUID and VSM results in this study. Comparing the remanent magnetization results obtained by conventional and molten salt methods (Figs. 7 and 8), reveals a lower remanent magnetization for the conventional sample (2.5 memu/g), which may be attributed to the smaller volume of secondary phase. This result is in agreement with results of Aurivillius thin films recently published elsewhere,[26] where thorough phase and microstructural analysis demonstrated the presence of magnetic $CoFe_{2-x}Ti_xO_4$ impurities at a volume fraction of 3.95%, which accounted for the entire measured magnetization in the $Bi_5Ti_3Fe_{0.7}Co_{0.3}O_{15}$ thin films and therefore demonstrated that these thin films are not single phase multiferroics at room temperature. Moreover, there is considerable evidence of phase separation between $CoFe_2O_4$ spinel phase and perovskite structures such as $BiFeO_3$, $BaTiO_3$, and $PbTiO_3$.[27–29] Similar separation also has been reported between $CoFe_2O_4$ spinel and the $Zn_{1-x}Mn_xO$ Wurtzite structure.[30]

Polarization-electric (PE) loops for the BFCT made from conventional method, which possesses the random orientation, show a high level of leakage, from dc conductivity. The leakage is far lower in the materials fabricated via molten salt, in Fig. 10(b). Such leakage may result from mixed valence Fe^{2+} and Fe^{3+} or oxygen vacancies and even both, as observed in $BiFeO_3$.[25] Note, however, that as the loops are not saturated, PE loops are unable to provide evidence of ferroelectricity in this case.

It is important to note, however, that although these materials contain unwanted secondary phase, it was possible to drive them to high electric fields, and in the case of conventionally prepared BFCT, butterfly loops are evident (Fig. 11(a)) at an electric field of 12 kV/mm. This provides strong evidence of both ferroelectricity and piezoelectricity, via the generation of negative strain. For the orientated sample (Fig. 11(b)) ferroelectricity from strain field is not evident, simple electrostriction at a drive field of 11 kV/mm.

V. CONCLUSIONS

BFCT with a high degree of texture has been produced by molten salt synthesis, which is strongly textured along the [002] direction. However 2% (by volume) of a Co–Fe spinel like secondary phase was identified by electron backscattering SEM imaging, and far lower in the material prepared by conventional processing. Magnetic characterization showed that the secondary phases dominate the ferromagnetic behaviour; in fact, a correlation can be made between the magnitude of the remnant magnetic polarization, and the concentration of secondary phase. The use of a textured ceramic allows us to categorically show that the observed isotropic ferromagnetic ordering is not associated with the orientated anisotropic Aurivillius phase, as confirmed by magnetic measurements in- and out-of-plane, and strongly suggests that this composition is not multiferroic. This result is in agreement with results on BFCT thin films recently published elsewhere.[26] Polarization-electric field measurements show a high level of conductivity in the conventionally prepared materials, and saturation was not possible in either sample types. Ferroelectricity has been confirmed for the conventional preparation route via the presence of a butterfly loop. The presence of the secondary phase has not significantly reduced the breakdown voltage of this system, of >11 kV/mm.

ACKNOWLEDGMENTS

The support of Science Foundation Ireland (SFI) under FORME Strategic Research Cluster Award number 07/SRC/I1172 is gratefully acknowledged. Also thanks to Dr. Faye Bygrave for her contribution in this paper.

[1]N. A. Hill, J. Phys. Chem. B **104**, 6694 (2000).
[2]I. Sosnowska, T. Peterlin-Neumaier, and E. Steichele, J. Phys. C **15**, 4835 (1982).
[3]B. Aurivillius, Ark. Kemi **1**, 499 (1950).
[4]L. G. V. Uitert and L. Egerton, J. Appl. Phys. **32**, 959 (1961).

[5]I. G. Ismailzade, V. Nesterenko, F. A. Mirishli, and P. G. Rustamov, Kristallografiya **12**, 468 (1967).
[6]X. Mao, W. Wang, X. Chen, and Y. Lu, Appl. Phys. Lett. **95**, 082901 (2009).
[7]F. K. Lotgering, J. Inorg. Nucl. Chem. **9**, 113 (1959).
[8]G. E. Lloyd, Miner. Mag. **51**, 3 (1987).
[9]J. Melngailis, J. Vac. Sci. Technol. B **5**, 469 (1987).
[10]A. Rafferty, T. Prescott, and D. Brabazon, Ceram. Int. **34**, 15 (2008).
[11]F. K. Lotgering, Philips Res. Rep. **11**, 337 (1956).
[12]G. Blasse, Philips Res. Rep. **18**, 383 (1963).
[13]K. Rao, A. Kumara, M. Varmaa, G. Choudary, and K. H. Rao, J. Alloys Compd. **488**, L06 (2009).
[14]R. A. McCurrie, *Ferromagnetic Materials: Structure and Properties* (Academic, 1994).
[15]S. Kawano, N. Achiwa, N. Yamamoto, and S. Higashi, Mater. Res. Bull. **11**, 911 (1976).
[16]E. K. Mooney, J. A. Nelson, and M. J. Wagner, Chem. Mater. **16**, 3155 (2004).
[17]J. G. Wan, X. W. Wang, Y. J. Wu, M. Zeng, Y. Wang, H. Jiang, W. Q. Zhou, G. H. Wang, and J. M. Liu, Appl. Phys. Lett. **86**, 122501 (2005).
[18]A. Franco, E. C. O. Lima, M. A. Novak, and P. Well, J. Magn. Magn. Mater. **308**, 198 (2007).
[19]J. B. Silva, W. d. Britoa, and N. D. S. Mohallem, Mater. Sci. Eng., B **112**, 182 (2004).
[20]I. Panneer Muthuselvam and R. N. Bhowmik, Solid State Sci. **11**, 719 (2009).
[21]L. Horng, G. Chern, M. C. Chen, P. C. Kang, and D. S. Lee, J. Magn. Magn. Mater. **270**, 389 (2004).
[22]J. A. Paulsen, C. C. H. Lo, J. E. Snyder, A. P. Ring, L. L. Jones, and D. C. Jiles, IEEE Trans. Magn. **39**, 3316 (2003).
[23]A. Franco and F. C. Silva, Appl. Phys. Lett. **96**, 172505 (2010).
[24]Z. X. Tang, C. M. Sorensen, and K. J. Klabunde, Phys. Rev. Lett. **67**, 3602 (1991).
[25]J. F. Scott, J. Phys.: Condens. Matter **20**, 0211001 (2008).
[26]L. Keeney, C. Groh, S. Kulkarni, S. Roy, M. E. Pemble, and R. W. Whatmore, J. Appl. Phys. **112**, 024101 (2012).
[27]R. Muralidharan, N. Dix, V. Skumryev, M. Varela, F. Sánchez, and J. Fontcuberta, J. Appl. Phys. **103**, 07E301 (2008).
[28]H. Zheng, J. Wang, L. Mohaddes-Ardabili, M. Wuttig, and L. Salamanca-Riba, Appl. Phys. Lett. **85**, 2035 (2004).
[29]J. Li, I. Levin, J. Slutsker, V. Provenzano, and P. K. Schenck, Appl. Phys. Lett. **87**, 072909 (2005).
[30]S. Gilliland, A. Segura, J. F. Sánchez-Royo, L. M. García, F. Bartolomé, J. A. Sans, G. Martínez-Criado, and F. Jimenez-Villacorta, J. Appl. Phys. **108**, 073922 (2010).